# A Theory of Post-Stall Transients in Axial Compression Systems: Part II—Application

**E. M. Greitzer**
Massachusetts Institute of Technology, Cambridge, MA

**F. K. Moore**
Cornell University, Ithaca, NY

*Using the theory developed in Part I, calculations have been carried out to show the evolution of the mass flow, pressure rise, and rotating-stall cell amplitude during compression system post-stall transients. In particular, it is shown that the unsteady growth or decay of the stall cell can have a significant effect on the instantaneous compressor pumping characteristic and hence on the overall system behavior. A limited parametric study is carried out to illustrate the impact of different system features on transient behavior. It is shown, for example, that the ultimate mode of system response, surge or stable rotating stall, depends not only on the* B *parameter, but also on the compressor length-to-radius ratio. Small values of the latter quantity tend to favor the occurrence of surge, as do large values of* B. *Based on the analytical and numerical results, some specific topics are suggested for future research on post-stall transients.*

## Introduction

In a companion paper, presented as Part I [1], a new theoretical approach was described for analysis of the types of post-stall transients that occur in multistage axial compression systems. An approximate solution procedure was developed, using a Galerkin technique, which led to a system of coupled, nonlinear, ordinary differential equations for the annulus averaged mass flow, the plenum pressure, and the rotating-stall cell amplitude, respectively.

In the present paper, we consider the application of these equations. We first examine their overall qualitative features. Following this, quantitative numerical results are presented for a representative low-speed compression system. These serve to illustrate not only the effects of various system parameters, but also some of the basic fluid dynamic phenomena that occur in the transients of interest. Finally, some recommendations are given concerning specific topics for research in the general area of stall recovery in aircraft gas turbine engines.

## Qualitative Features of the Transient System Behavior

Before considering specific cases of interest, it is useful to examine the general features of the simplified equation set developed in Part I (equations I.59, 60, 61).[1] As mentioned there, these equations can be reduced to those describing either pure surgelike (i.e., purely one-dimensional) transients, or pure rotating stall, and permit the existence of pure modes, that is, either surge or rotating stall without the other.

A physically relevant question, however, is whether such modes could evolve from initial small disturbances. This question was touched on in Part I, and it was suggested that finite amplitude rotating stall cannot evolve without producing a finite disturbance in $\Phi$ or $\Psi$, although for small values of $B$, the disturbance can be a noncyclic transient. Equations (I.59–61), in fact, suggest that if $B$ is small and the throttle is steep, $\Phi$ may remain essentially constant while $J$ and $\Psi$ vary with time. In this limiting case, the solution of equation (I.61) is:

$$\frac{J}{J_e} = \frac{1}{1+\left(\frac{J_e}{J_0}-1\right)\exp\left(-\frac{3aJ_eH/W}{4(1+ma)}\xi\right)} \tag{1}$$

where $J_0$ is an assumed initial disturbance. $J$ thus grows steadily from $J_0$ to a final, fully developed pure rotating-stall value of $J_e$, defined in equation (I.62).

Figure 1 shows this behavior for the compressor geometry

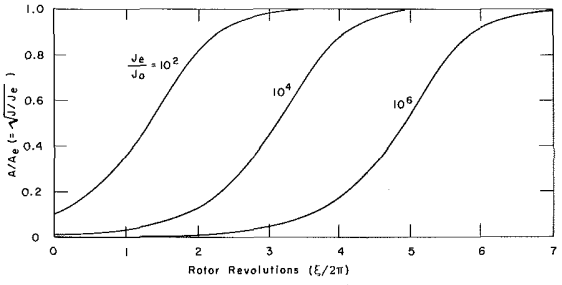


**Fig. 1 Growth of (normalized) stall-cell amplitude at constant mass flow ($m$ = 1.75, $H/W$ = 0.72, $1/a$ = 3.5); curves from equation (1)**

[1] Equations given in Part I will be denoted by roman numeral prefixes.

Contributed by the Gas Turbine Division of THE AMERICAN SOCIETY OF MECHANICAL ENGINEERS and presented at the 30th International Gas Turbine Conference and Exhibit, Houston, Texas, March 18-21, 1985. Manuscript received at ASME Headquarters, January 10, 1985. Paper No. 85-GT-172.

discussed in Part I. For reference, the relevant parameters are: $m = 1.75$, $H = 0.18$, $W = 0.25$, $1/a = 3.5$. The calculations have been done for $\Phi = 0.25$ and three different values of $J_e/J_0$: $10^2$, $10^4$, and $10^6$.

The graph shows the normalized rotating stall amplitude, $A/A_e$ $(= \sqrt{J/J_e})$, versus time, with time being plotted in rotor revolutions. It is clear from the figure that the growth is dependent on the initial conditions. This can be seen from equation (1) which, if $J_0 \ll J_e$, can be written for small times as:

$$J - J_0 = J_0 \left( \frac{3aJ_eH/W}{4a(1+ma)} \right) \xi + \ldots \tag{2}$$

i.e., the increment of $J$ is proportional to the initial value. However, once the value of $J$ has grown enough that the nonlinear aspects of the process become important, the approach to the final amplitude becomes independent of the initial conditions. This type of behavior, which is typical of nonlinear systems, will also be encountered later, when we discuss the results for the combined rotating stall and surge transients.

**Small Axisymmetric Disturbance to Finite Amplitude Rotating Stall.** We know that our equations permit both pure surge and pure rotating stall. We can also inquire whether those "pure" motions are stable to disturbances of the other family. First, consider the case of fully developed rotating stall subject to weak axisymmetric, (i.e., surgelike) disturbances. For the limiting case of an infinitely steep throttle line, we obtain a harmonic-oscillator equation for $\Phi(\xi)$, with the coefficient of the damping term given by

$$\text{damping coefficient: } -\frac{3}{2}\left[1 - \frac{1}{2}J - \left(\frac{\Phi}{W} - 1\right)^2\right]\frac{1}{W} \tag{3}$$

The damping would be negative if $J$ were zero. If the stall is fully developed, however, $J$ is $J_e = 4\{1 - [(\Phi/W) - 1]^2\}$, and the damping coefficient becomes

$$\text{damping coefficient: } \frac{3}{2}\left[1 - \left(\frac{\Phi}{W} - 1\right)^2\right]\frac{1}{W} \tag{4}$$

which is positive. We thus conclude that small-disturbance surge-type oscillations tend to be damped in the presence of equilibrium rotating stall. This might also be inferred from the fact that the relevant compressor curve is now the negatively sloped fully developed rotating-stall curve.

**Small Angular Disturbance of Surge.** The converse situation is that of a finite amplitude axisymmetric (surge) oscillation subjected to a small rotating-stall-like disturbance. Equation (I.61) governs the growth or decay of $J$. During the surge oscillation, $\Phi$ is varying so that the bracket in equation (I.61) may be either positive or negative, and it is therefore not obvious whether $J$ will have a net growth.

To examine this in the limiting case of an infinitely steep throttle, one may show that the pure surge equation in this case takes the same form as equation (I.48) for rotating stall, with the time variable $\xi/(2Bl_c)$ playing the role of $\theta^*$. We may thus infer from equations (I.53, 62) that the corresponding Galerkin solution is:

$$\Phi - \bar{\Phi} = W J_e(\bar{\Phi}) \sin\left(\frac{\xi}{2Bl_c}\right) \tag{5}$$

Using this in (I.61), and neglecting terms of order $J^2$, gives a linearized equation for $J$:

$$\frac{1}{J}\frac{dJ}{d\xi} = \frac{3aH/W}{1+ma}\left[-\frac{J_e}{4} - 2\sqrt{J_e\left(1 - \frac{J_e}{4}\right)}\sin\left(\frac{\xi}{2Bl_c}\right) + \frac{1}{2}J_e\cos 2\left(\frac{\xi}{2Bl_c}\right)\right] \tag{6}$$

The solution is:

$$\frac{J}{J_0} = \exp\frac{3aH/W}{1+ma}2Bl_c\left[-\frac{J_e}{4}\frac{(\xi - \xi_A)}{2Bl_c} + 2\sqrt{J_e\left(1 - \frac{J_e}{4}\right)}\cos\left(\frac{\xi}{2Bl_c}\right) + \frac{J_e}{4}\sin 2\left(\frac{\xi}{2Bl_c}\right)\right] \tag{7}$$

where a constant of integration $\xi_A$ is included. The question is whether $J$ is greater or less than its initial value $J_0$.

If the square bracketed term in equation (7) is positive, $J > J_0$, while if it is negative, $J < J_0$. The first term in the square bracket, being negative and increasing, represents a tendency for $J$ to be progressively smaller than $J_0$ for large time; however, the oscillatory harmonic terms could reverse that tendency for early or moderate times.

Figure 2 illustrates the possibilities for the special case of $\bar{\Phi}/W = 1$ $(J_e = 4)$. In this case the square bracket takes the form:

$$\text{overall growth factor: } \left[-\frac{\xi - \xi_A}{2Bl_c} + \sin 2\left(\frac{\xi}{2Bl_c}\right)\right] \tag{8}$$

## Nomenclature

$A_e$ = amplitude of first-harmonic angular disturbance in pure rotating stall, $\sqrt{J_e}$
$A_c$ = compressor duct area
$a$ = reciprocal time-lag parameter of blade passage
$a_s$ = sound speed
$B$ = $(U/2a_s)\sqrt{V_p/A_cL_c}$
$f_0$ = nondimensional propagation speed of rotating-stall-like disturbances
$H$ = semi-height of cubic characteristic
$J$ = square of amplitude of angular disturbance of axial-flow coefficient
$J_0$ = initial value of J
$J_e$ = value of J for fully developed rotating stall at the existing average axial-flow coefficient
$K_T$ = parabolic throttle coefficient
$L_c$ = total effective length of compressor and ducts
$l_c$ = total length of compressor and ducts, in wheel radii
$m$ = downstream duct-flow parameter
$U$ = wheel speed at mean diameter
$V_p$ = volume of plenum
$W$ = semi-width of cubic characteristic
$\xi$ = time, referred to time for wheel to rotate one radian
$\xi_e$ = dimensionless time for development of equilibrium rotating stall
$\xi_A$ = defines time of start of angular disturbance
$\Phi$ = axial flow coefficient, averaged over angle (axial velocity divided by wheel speed)
$\bar{\Phi}$ = flow coefficient averaged over both angle and time
$\Phi_T$ = flow coefficient of throttle duct, referred to entrance-duct area
$\phi$ = local axial velocity coefficient (local axial velocity divided by wheel speed)
$\Psi$ = total-to-static pressure-rise coefficient (inlet to plenum)
$\psi$ = pressure-rise coefficient, $\Delta P/\rho U^2$
$\psi_c$ = axisymmetric pressure-rise coefficient
$\psi_{c_0}$ = shut-off head coefficient

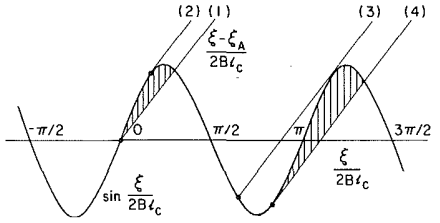


Fig. 2 Amplitude of rotating stall during a surge cycle, as indicated by terms in equation (8), with $\Phi = W$; different choices of $\xi_A$ provide different starting points; net amplification occurs in shaded zone

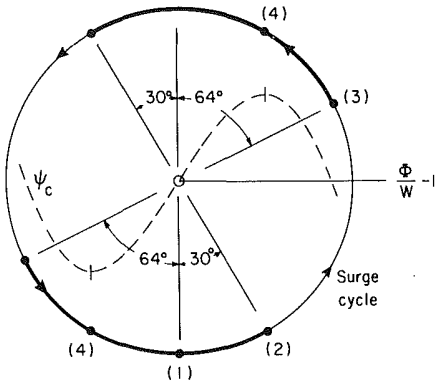


Fig. 3 Sketch of surge cycle showing regions in which net growth of rotating stall can occur; numbered points correspond to lines of Fig. 2

The first and second terms of this expression are plotted separately on Fig. 2. A series of lines are shown to represent the first term, because $\xi_A$ is arbitrary. Where any one of these lines cross the sine wave is a possible starting time for the disturbance. What happens after the starting time clearly depends on the phase of the sine wave (surge oscillation) when the angular variation starts. If the start is at $\xi = 0$, then the shaded area above line (1) shows the duration and intensity of the excursion of $J$, although whether the amplification is sufficient for rotating stall to develop cannot be found from this small-perturbation solution.

If the intersection point is moved along the sine wave, the time available for amplification shortens, until line (2) is reached for which there can be no growth at all. Not until line (3) is reached does amplification again become positive. The greatest overall growth of the rotating stall is found for line (4).

To visualize these results in a different manner, we sketch on Fig. 3 the axisymmetric compressor characteristic, and overlay a surge cycle sketched as a counterclockwise circle centered at $\beta = 0$. The heavy lines indicate phase zones in which initial angular disturbances will at least briefly amplify.[2] Outside those zones, overall growth of a weak angular disturbance cannot occur. Points are labeled on Fig. 3 to show correspondence with the lines of Fig. 2.

The foregoing discussion indicates that it is important to know the character of an initial disturbance and the timing of its introduction, whether it is velocitylike or pressurelike, and its magnitude. All those factors can have an effect on the ultimate trajectory of the disturbance.

**Summary of Qualitative System Behavior.** Before presenting the numerical results for the trajectories in $\Phi$, $\Psi$, and $A$ space, we can summarize certain expectations about the system behavior:

1 Pure modes of either surge or rotating stall are permitted as permanent oscillations.

[2] Note that the growth we are describing is the overall value; the local growth rate is just dependent on the slope of the compressor characteristic and is positive at all points where the compressor has a positive slope.

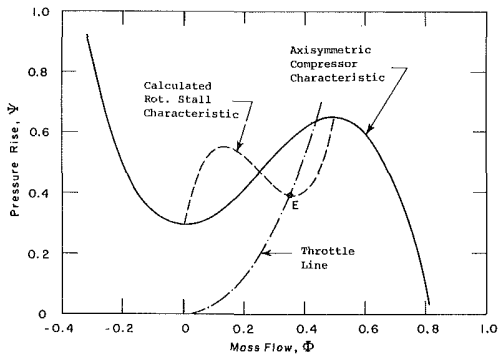


Fig. 4 Compressor and throttle characteristics ($H/W = 0.72$ and $\psi_c/H = 1.67$)

2 Pure surge can evolve from an initial weak axisymmetric disturbance.

3 In general, a weak angular disturbance will not produce pure rotating stall, but will produce some degree of axisymmetric disturbance.

4 The initial growth rate of an angular disturbance (toward a limit cycle value) depends on the strength of the initial disturbance, but becomes independent of this when the nonlinear aspects of the process become important.

5 Angular disturbances will grow toward an equilibrium value depending on the instantaneous flow coefficient; if the latter is also changing with time, angular-disturbance amplitude "chases a moving target."

6 Excursions of flow coefficient will tend to suppress angular variations, and the presence of angular variations will tend to suppress surge.

7 For the compressor characteristic examined, any small surgelike disturbances in the presence of fully developed rotating stall will tend to decay.

8 In the presence of fully developed surge, a small angular disturbance may decay or may grow (but only during a fraction of one surge cycle), depending on the phase of the surge cycle in which the disturbance originates.

## Numerical Results for General Post-Stall Transients

The set of coupled ordinary differential equations given as equations (I.59), (I.60), and (I.61) have been solved numerically for a representative set of parameters to show some of the basic features of the phenomena. Specifically, calculations have been carried out to illustrate the effects of the nondimensional parameters $B$ and $l_c$ as well as of the initial conditions. In view of the approximate nature of the approach taken, however, it is to be emphasized that no extensive parametric study has been performed.

In the calculations, the axisymmetric compressor characteristic has been taken to be the same cubic curve described in Part I, with the parameters used in Chue's calculations [1]; this is shown for reference as the solid line in Fig. 4. The throttle curves are taken as parabolas. The one shown as the dash-dot line in the figure corresponds to $K_T = 6.5$, for which most of the calculations were carried out; other throttle settings used are noted in the text. As mentioned in Part I, these curves are representative of a three-stage, low-speed compressor, somewhat similar to that used in [2].

Unless specified, the initial values of nondimensional pressure rise and flow coefficient are taken to be the values at the peak of the curve, i.e., $\Phi = 0.5$ and $\Psi = 0.66$, for the particular characteristic chosen. At that condition, we shall impose a level of circumferential nonuniformity defined by $A(0)$ at time $\xi = 0$ (recalling that the nondimensional amplitude of the $\theta$ dependent velocity nonuniformity is $AW$, and $A \equiv \sqrt{J}$). The system of equations (I.59-61) governs the

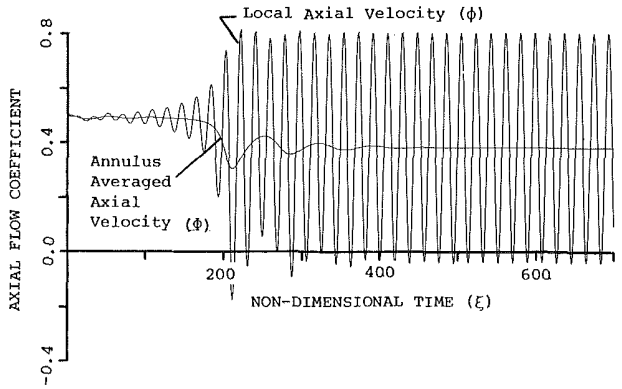


Fig. 5(*a*) Time history of local and annulus-averaged axial velocity coefficient during transient to rotating stall

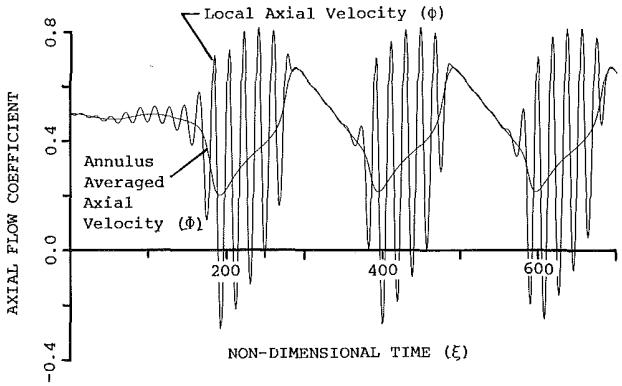


Fig. 5(*b*) Time history of local and annulus-averaged axial velocity coefficient during transient to surge

ensuing transient which, due to the coupling, shows either temporal (surgelike) or circumferential (rotating-stall-like) variations.

**Compressor and Compression System Transient Behavior in Surge and Rotating Stall.** To introduce the quantitative results, we show the transient behavior for two situations: one in which the outcome is rotating stall and one in which it is surge. These are illustrated in Figs. 5(*a*) and 5(*b*). The figures show the nondimensional annulus averaged and local axial velocity (i.e., the axial velocity that would be measured by a hot-wire probe at the compressor inlet) versus nondimensional time in rotor revolutions. The local velocity is given by the following expression obtained by combining equations (I.52, 53, 57):

$$\phi = \Phi(\xi) + WA(\xi)\sin(\theta - f_0\xi) \tag{9}$$

The two calculations correspond to a throttle setting of $K_T$ = 5.5, and to values of $B$ of 0.5 and 1.0, respectively. In the calculations, the value of $l_c$ was 8.0 and the initial rotating stall amplitude $WA(0)$ was 1% of the average velocity (nondimensional amplitudes of axial velocity perturbation of 0.005). In addition, the minimum value of axial velocity nonuniformity occurring at any subsequent time during the transient was set equal to the initial value; this seems more physically realistic than letting this quantity decrease to zero.

It can be seen that the resulting instantaneous velocities are very similar to those seen in the time traces than one obtains during compressor transients (e.g., [2]). In particular, the growth and decay of the stall cell as the compressor mass flow goes in and out of the stalled flow regime is very evident. What may be less evident from this time-domain representation, but will be shown in the subsequent figures, is that this growth and decay of the stall cell does not occur in a quasi-steady manner, and that the instantaneous compressor

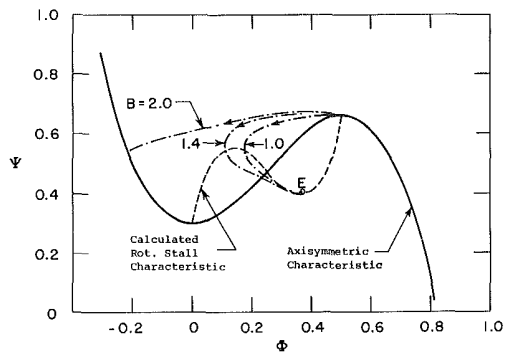


Fig. 6 Transient compression system response (Ψ versus Φ) for different values of $B$ ($l_c$ = 8.0, $A(0)W$ = 0.005)

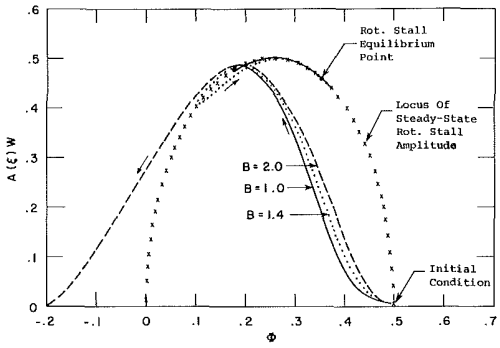


Fig. 7 Evolution of rotating-stall amplitude during system transient; effect of $B$ parameter ($l_c$ = 8.0, $A(0)W$ = 0.005)

performance does not therefore correspond to the steady-state rotating-stall characteristic.

**Effect of $B$ Parameter.** Although Fig. 5 gives one illustration of the (familiar) effect of the $B$ parameter, Fig. 6 shows this in more detail. In the figure, the transient system response is presented in terms of the overall pressure rise (atmosphere to plenum) and annulus-averaged flow coefficient for three different values of $B$: 1.0, 1.4, and 2.0. Also indicated is the axisymmetric curve (the solid line) and the calculated rotating stall curve (dashed). The values of $l_c$ and $WA(0)$ are the same as for Fig. 5. The throttle setting is that illustrated in Fig. 4, $K_T$ = 6.5. Note that, at this throttle setting, the surge included an appreciable portion of reversed flow contrary to the situation shown in Fig. 5 (deep surge versus classic surge, in the terminology of [2] and [3]).

As expected, higher values of $B$ cause larger excursions in axial velocity. At the highest value, this would lead to surge cycles, whereas for the lower values, the eventual result of the initial transient is operation at a new equilibrium point on the rotating-stall curve.

The picture shown in Fig. 6 is a somewhat familiar one. However, Fig. 7 presents a new, more detailed view of these same transients. This figure shows the rotating-stall amplitude, $A(\xi)W$ ($= \sqrt{J}W$), versus annulus-averaged flow coefficient ($\Phi$) for the same conditions. Also indicated in the figure is the locus of steady-state rotating-stall amplitudes for different values of $\Phi$, i.e., the amplitude for steady-state operation at that mass flow. This is just the value calculated from equation (I.62), which has a maximum at $\Phi$ = 0.25 and goes to zero (i.e., steady-state rotating stall ceases) at $\Phi$ = 0.5 and $\Phi$ = 0.0. This curve represents the locus of equilibrium states toward which rotating-stall-like disturbances must tend.

An obvious feature of the transients is that over the first part (for $\Phi$ greater than roughly 0.25) the amplitude is substantially less than that during steady-state operation. For lower flows, however, the amplitude can actually exceed the

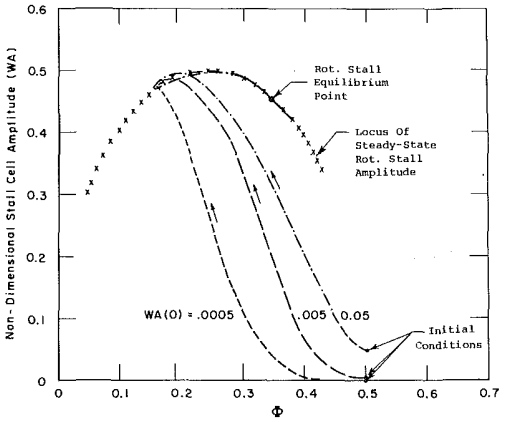


Fig. 8 Evolution of rotating-stall amplitude during system transient; effect of initial conditions ($l_c$ = 8.0, $B$ = 1.0)

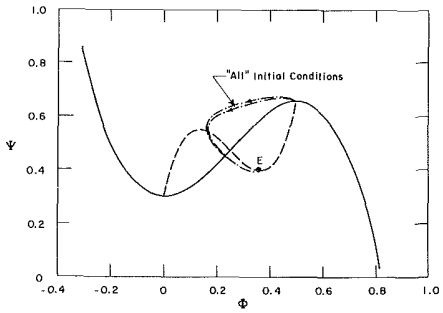


Fig. 9 Transient compression system response; effect of initial conditions ($l_c$ = 8.0, B = 1.0)

steady-state value. Further, as seen in the curve for $B$ = 2.0, the rotating stall persists into the reverse-flow regime during the transient. This can be contrasted with steady-state operation in which (for this compressor) rotating stall cannot exist when flow is reversed.

It should be noted that when the transient leads to surge cycles, calculations have only been carried out for part of the initial cycle. The reason is that the calculated stall-cell amplitude decays to a very low value during the extended operation at reverse flow. Thus the "initial condition" for the part of the transient when the flow through the compressor accelerates (from zero) back to unstalled operation is essentially that of zero stall-cell amplitude. Under these conditions, as discussed above, there will be no subsequent growth of rotating stall, and the transient will proceed as pure surge.

It does not seem physically realistic, however, that there would be a lower level of flow asymmetry during a surge cycle than during operation prior to stall, and thus this part of the calculation does not appear to be a valid description. As done in the calculations leading to Fig. 5, it might be more correct to say that there is always some minimum disturbance amplitude present, able to provide an "initial disturbance" at any time. In view of the lack of information about this point, however, we have not elected to do this, but rather to restrict computations to the first part of each transient. We will return to a discussion of this point in the next section.

A basic feature shown in Figs. 5 and 7 is the growth and decay of the rotating stall as the mass flow varies, an effect anticipated in Figs. 2 and 3 and the related discussion. That this process must actually occur has been known qualitatively for some time. As far as the authors know, however, this is the first time that it has been calculated, in even an approximate manner, using the equations of motion for nonaxisymmetric flow in a compressor.

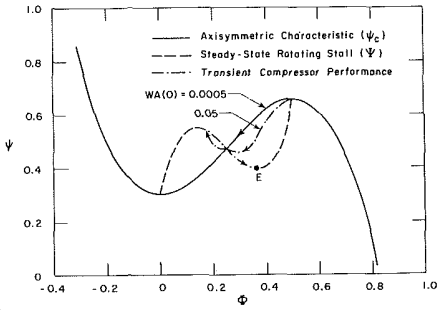


Fig. 10 Instantaneous compressor pumping characteristic during system transient; effect of initial conditions ($l_c$ = 8.0, $B$ = 1.0)

**Effect of Initial Conditions.** Effects of initial level of disturbance, $A(0)W$, have also been examined. The results are given in Fig. 8, which show the compressor treatment in an $AW$, $\Phi$ (rotating-stall amplitude, flow coefficient) plane. The calculations shown are for $B$ = 1.0, $l_c$ = 8.0, and for three different initial values of axial velocity nonuniformity: 0.05, 0.005, 0.0005; these correspond to initial perturbations of 10%, 1%, and 0.01% of the mean axial velocity. The last of these is roughly the size that would be expected in a good wind-tunnel test section, and the first appears to be larger than the (long-wavelength) velocity disturbances generally seen prior to rotating stall. Thus, the range of initial disturbance amplitude conditions encompasses essentially all physically plausible situations. The value regarded as the "base case," the 1% level, might be a reasonable estimate for the magnitude of velocity nonuniformities to be expected prior to rotating stall, but there seem to be few data on this point. In the figure, the locus of steady-state rotating stall amplitude is again indicated (by the crosses) as is the eventual equilibrium point in rotating stall, at $\Phi$ = 0.35, $\Psi$ = 0.455.

The effect of the initial conditions is strong early in the transient, since the growth rate is proportional to the amplitude of the perturbation. After the stall amplitude has reached a certain size, however, on the order of 0.1-0.2, nonlinear effects become important, and the slope of the trajectory is no longer set primarily by initial conditions. Although there are some differences in the extent of the excursion in axial velocity between the three cases, the behavior once the trajectory approaches the vicinity of the steady-state locus is fairly similar for the three cases. As stated earlier, this relative independence from the initial conditions during the approach to the equilibrium state is typical of nonlinear systems of the type which we are examining.

The effect of initial conditions can also be shown in a $\Phi$, $\Psi$ representation, as in Fig. 9, where curves for initial amplitudes 0.05 and 0.0005 are shown. Even though there are two orders of magnitude difference between the initial values, the trajectories of the plenum pressure versus flow coefficient are not at all dissimilar; they both show roughly the same excursion in mass flow before ending up at the eventual equilibrium point in rotating stall, denoted on the graph by $E$.

The influence of initial conditions on the compressor pumping characteristic, i.e., the instantaneous compressor output, can also be examined. The instantaneous output can be found by subtracting the momentum changes in the compressor duct from the overall (atmosphere to plenum) pressure rise. The result is presented in Fig. 10, which gives instantaneous compressor pressure rise versus instantaneous annulus-averaged axial velocity parameter, for the same conditions as in Fig. 9, namely $B$ = 1.0, $l_c$ = 8.0, and initial amplitudes $WA(0)$ = 0.0005 and 0.05.

The trajectory for the former can be seen to follow the axisymmetric characteristic until near $\Phi \sim 0.25$ (the point of maximum steady-state rotating stall amplitude), then depart and verge towards the steady-state rotating-stall curve. The trajectory for 0.05 departs from the axisymmetric curve

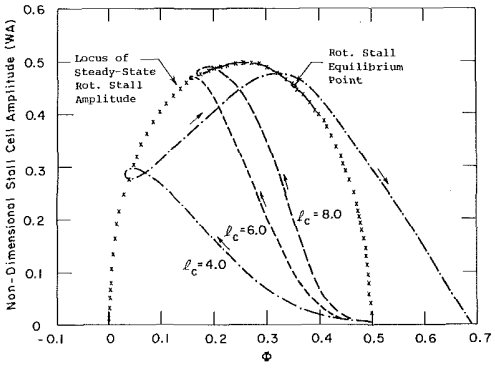


Fig. 11 Evolution of rotating stall amplitude during system transient; effect of length-to-radius ratio ($A(0)W = 0.005, B = 1.0$)

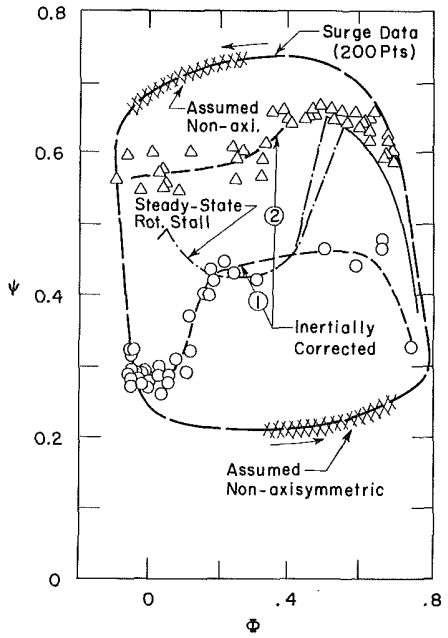


Fig. 12 Instantaneous compressor pumping characteristic derived from surge cycle data (from [4]); measured steady-state rotating stall curve also shown for reference ($B = 1.58, l_c = 8, A(0)W = 0.005$)

virtually from its initial point and tracks essentially along the steady-state rotating-stall curve after it first passes through $\Phi = 0.25$. The eventual equilibrium point is again indicated in the figure as $E$.

Calculations have also been carried out for other values of $B$ to examine the effect of initial conditions. These confirm, in general, the trends shown in the preceding figures, namely that over a fairly wide range of initial conditions, the results do not depend strongly on the precise values used. There are, however, situations in which the initial condition can make a great deal of difference in the eventual outcome. For example, if one is on the "borderline" with regard to encountering surge or rotating stall, a change in the initial amplitude can alter the system behavior, from tending to an equilibrium point to undergoing a surge cycle. The range of situations in which the initial condition had a significant effect on the ultimate result was not investigted in any detail. From the few studies that were done, it appears that if $B$ differs by more than about 10% from the transition value, the influence of the initial condition is substantially diminished. As suggested above, the possible influence of initial conditions, and thus the question of how to specify initial conditions properly (as well as the details of the nature of disturbances at different stages of the surge cycle), is a topic that must be investigated further.

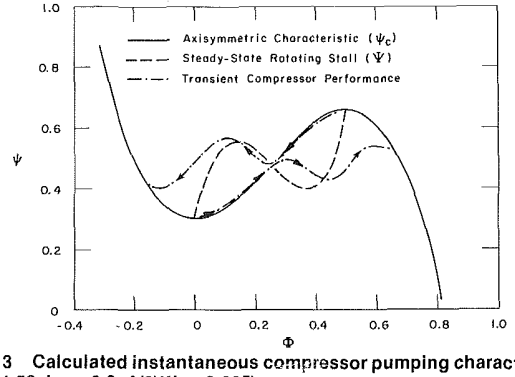


Fig. 13 Calculated instantaneous compressor pumping characteristic ($B = 1.58, l_c = 8.0, A(0)W = 0.005$)

Note that one *can* produce changes in computed system behavior by making sufficient changes of initial conditions. For example, if the initial amplitude is decreased to 0.00005 (0.01% of mean velocity), the growth of the rotating-stall cell is so slow during the transient that the compressor behavior is virtually on the axisymmetric curve throughout, and surge occurs. As discussed previously, however, it is felt that this represents an unrealistically weak initial disturbance, and it thus appears that the calculations may not be very sensitive to the initial conditions, although the matter clearly deserves more study.

**Effect of Compressor Length to Radius Ratio.** The other parameter investigated was $l_c$, the compressor length-to-radius ratio, and Fig. 11 shows trajectories for values of $l_c$ of 4.0, 6.0, and 8.0. The value of $B$ is 1.0 and the initial amplitude is $A(0)W = 0.005$ As in previous figures, the steady-state and equilibrium values of rotating stall amplitude are also indicated.

The curves for $l_c = 8.0$ and 6.0, while quantitatively different, have the same qualitative features, namely an initial rapid rise in amplitude and then a nearly quasi-steady motion along the steady-state amplitude curve until the equilibrium value is reached. A different situation exists for $l_c = 4.0$, however. There is a large difference between the unsteady trajectory and the steady-state curve and the system does not settle down to a new equilibrium point. Starting from initial conditions, the mass flow decreases then increases again and the stall-cell amplitude decays to a low value as the compressor returns to the unstalled portion of the compressor characteristic. This would thus indicate surge cycles, rather than an approach to equilibrium in rotating stall.

These calculations show that, in addition to the $B$ parameter, the length-to-diameter ratio, $l_c$, can also affect whether a given system will exhibit surge or rotating stall. The physical reason is that, for the same value of $B$, a decrease in length-to-radius ratio means that the time for the formation of a rotating stall cell becomes relatively longer in proportion to the time for a mass flow excursion so that the instantaneous characteristic is more like the axisymmetric characteristic.

It is also relevant to briefly relate these calculations to previous studies. In [2], the only effect investigated was the influence of the $B$ parameter. In the published results, the "time constant" that characterized the rotating-stall formation time was kept constant at two rotor revolutions, since the available data was insufficient to determine it more precisely. (It was, however, stated that some calculations had been carried out using different values of that time constant and the results for the critical value of $B$ were somewhat different, although over the range examined the difference was not great.) In the present study, there is no need to assume such a time constant, because the manner in which the compressor output transitions from axisymmetric to fully developed rotating stall is not calculated.

**Comparison with Data on Instantaneous Compressor Performance.** In addition to examining the impact of $B$ parameter, initial conditions, and compressor length-to-radius ratio, the present calculation procedure has also been used to help interpret transient compressor data. Specifically, data from a surge cycle, in the form of overall atmospheric to plenum pressure rise versus mass flow, has been used to form an estimate of the instantaneous compressor pumping characteristic.

The procedure originally followed [4, 5] was to subtract from this overall pressure rise a one-dimensional (i.e., axisymmetric) correction for the inertial forces due to fluid accelerations during the surge cycle. The explicit expression for the correction is:

$$\psi_c = \Psi + l_c \frac{d\Phi}{d\xi} \tag{10}$$

The terms given by the data are $\Psi$ and $l_c\, d\Phi/d\xi$, $\psi_c$ being calculated; details of the procedure are given in [4, 5].

In applying this procedure, it is necessary to examine the (compressor inlet) time-resolved data to determine whether the flow is indeed axisymmetric. It was found that the data showed rotating stall, not fully developed, toward the end of each period of rapid flow change. Although the information is not sufficient to resolve all the details of the flow, the conclusion is that axisymmetric flow cannot be assumed for the entire surge transient that the data represents. The present theory, however, provides a means to calculate the effect of this departure from axisymmetry (perhaps most dramatically illustrated in Fig. 5(*b*), and thus to aid in extracting the axisymmetric characteristic from this type of transient.

A sample of the data is shown in Fig. 12, with the inertially corrected characteristics determined by equation (10). The triangles and the circles denote the values obtained for the decelerating and accelerating portions of the surge cycle; curves 1 and 2 have been fitted through these points. The dot-dash line is measured data for steady-state rotating stall operation. It can be seen that even though there is some scatter in the calculated $\psi_c$, due presumably to the differentiation of the experimental data, the points fall into two categories: For decelerations, the corrected curve lies substantially above the steady-state rotating-stall curve, whereas for accelerations (at least for $\Phi > 0.4$), the derived pumping characteristic is considerably below the steady-state curve. In view of this behavior, the question arises whether a single-valued axisymmetric curve is indeed a valid representation, or whether a more complex axisymmetric behavior must be invoked.

To examine this matter from the point of view of the present theory, calculations have been carried out using the system parameters that characterize the transient data: $B = 1.58$, $l_c = 8.0$, and throttle curve $C$ (see Fig. 3). The calculations were done for both accelerating and decelerating flows. For the decelerations, initial conditions were $\Phi = 0.5$, $\psi = 0.66$, and $A(0)W = 0.005$. For the accelerating part of the cycle initial conditions were $\Phi = 0.0$, $\Psi = 0.3$, and $A(0)W = 0.005$.

The results are shown in Fig. 13. The solid line is the axisymmetric characteristic and the dashed line is the steady-state rotating stall curve. The computed instantaneous compressor performance (which corresponds to the quantity shown dashed in Fig. 12) is indicated by the heavy dash-dot lines. The arrows showing the direction of motion of the operating point should be carefully observed.

It can be seen that the computed and the experimental curves have strong similarities, at least qualitatively. In particular, the tendency for the compressor pumping characteristic to be above the axisymmetric performance in the reverse flow region and below it at high forward flows is clearly manifested.

The reason for this is found from consideration of the growth and decay of the rotating stall. During the latter part of the deceleration, the instantaneous rotating-stall amplitude is much larger than the steady-state value (which is zero for negative values of $\Phi$) and the compressor output is thus increased, compared to the axisymmetric value. During the acceleration, for the flows greater than $\Phi = 0.4$, say, the rotating stall amplitude is again much larger than that in steady-state operation, so the performance (i.e., pressure rise) is decreased compared to the axisymmetric value.

The main points in the foregoing comparison of experimental data with the present computations are thus:

1 The behaviors of the two are qualitatively similar, and
2 The departure of the compressor pumping characteristic from both axisymmetric and steady-state performance arises because the instantaneous rotating stall amplitude differs considerably from the steady-state value. In particular, in the latter part of both deceleration and acceleration processes, the stall cell is much larger than one would presume from steady-state considerations.

## Discussion of the Present Model and Suggestions for Future Work

Although the analysis and numerical calculations have pointed out certain features of the general transient which appear to be important, it is clear that the present treatment has only made a start on this very complex problem. It is thus appropriate to give some discussion about the aspects of the actual flow that are included in the theory, the aspects that are potentially important but have not been included, and the areas that have been mentioned as needing further investigation.

We can start by listing those aspects of the unsteady compressor and compression system behavior that are accounted for:

1 System dynamic characteristics: These are analyzed in a lumped parameter fashion. For the situations considered in the present report (low Mach number and low frequency) this is a very good approximation. As either frequency or Mach number is increased, one may have to adopt a more complex description of these components. In particular, there is, for high-pressure ratio compressors, the possibility of mass storage within the compressor itself so that a simple representation of the inertance of the flow in the compressor duct may not suffice. In this regard, however, it is of interest to note that Mani [6] has achieved some quite reasonable comparisons with experiments using very simple representations of the system parameters.

2 Inlet flow field: A description of the upstream flow is included in the theory. The flow upstream of the compressor is modeled as two-dimensional and unsteady, but irrotational. The upstream annulus is taken as having constant area, although this assumption can be relaxed, if necessary. It is not clear how valid the irrotationality assumption is, and this is a subject for investigation. Data are scarce on this point, although the results of Day [7] give some credence to this assumption.

Perhaps more serious is the assumption that axial and circumferential disturbances are related as they would be if they were harmonic. This assumption requires evaluation, as does that regarding entrance to the inlet guide vane as accomplished without head loss.

3 Exit flow field: A linearized description of the exit flow field is included in the theory. It is clear that the assumption of linearity in the exit static pressure perturbations cannot be correct in general, although the degree to which it is in error and, more importantly, its effect on the predictions of the theory is not obvious. Previous theories of steady-state

rotating stall, in particular [8] and [9] which have used this assumption, have had good success with predicting at least some of the features of the stall cell flow field.

4 The model of the throttle characteristic that is included is quite adequate for low-pressure ratios. For higher-pressure-ratio systems, there should be no problem with introducing a compressible version of this, as was done by Wenzel [10].

5 Throttle transients have not been included in the present calculations, but are within the scope of theory. There should be no difficulty in applying the theory to account for these. This is of interest since it has been found that throttle transients can have a significant effect on system behavior.

6 System hysteresis appears naturally in the theory since it is set by the stability of the system at the various intersection points of throttle and compressor curves. When closing the throttle (into stall) the compressor curve is the axisymmetric one. When opening the throttle from operation in fully developed rotating stall, the compressor curve is the rotating-stall one. There can thus be a difference in the throttle settings at which transition from unstall to stall and from stall to unstall occur.

7 Compressor geometry is represented by the axisymmetric characteristic.

8 Unsteady blade row response (internal aerodynamic lag of the compressor) is included in the theory. It is done in a rudimentary manner, because at present one does not know how much detail is needed to provide a satisfactory description.

From the above, it does appear that the basic elements that one might think necessary for an analytical description of general post-stall transients have been included. Having said this, however, it should be emphasized that their inclusion has, in some instances, been done in a quite approximate manner, with an impact on the overall prediction which is not well understood. In this connection, we can refer back to the analytical framework [8] on which this study is based. The equations developed there will always result in axial velocity profiles that are like those shown in Figs. 5(*a*, *b*) of Part I, rather than the "top-hat" type of profile that seems to be more characteristic of compressors that operate in rotating stall. At present, the reason for this discrepancy is unclear, but the fact that it exists suggests that there are aspects of the theory which should be improved, even for low-speed, low-pressure-ratio situations.

We have described those features that are included, and we now turn to others which we think will be important to include for problems of practical interest.

1 Effects of compressibility on compressor performance and inlet and exit flow fields.
2 Front-to-rear mismatching effects due to off-design operation in the compressor.
3 Heat addition in the burner.
4 Effects of inlet flow distortion.
5 Engine matching effects (nonconstant speed, for example).
6 Other compression system components.
7 Steady-state hysteresis in the axisymmetric compressor characteristic, if such exists.

Research is necessary to elucidate the influence of the effects named above. In addition to these, however, there are other topics that must be explored if one is to improve the quantitative capabilities of the theory. The first of these is the development of more exact methods for the calculations. The numerical results given in the present report are based on a one-term Galerkin procedure (equations (I.59–61)); as mentioned, this was all that could be carried out in the limited time available. However, the types of phenomena that are being investigated would appear to be very well suited for spectral or pseudospectral calculation methods [11], which might be applied, for example, to equations (I.42–44).

Another matter of concern is the rotating stall performance. The question of the behavior of the compressor at or near the point of instability is by no means settled. The present theoretical analysis predicts that the flow in the compressor will become unstable at the peak of the steady-state pressure rise curve. In practice, compressors are observed to become unstable on the negatively sloped part of the curve. While interstage (one-dimensional), volume effects have been invoked as a possible cause for this in high-pressure-ratio compressors, the behavior is observed at low pressure ratios also, and here the interstage effects are very small. Both experimental and theoretical research is needed on this topic.

The effect of inlet conditions has been mentioned before, and the point will not be belabored here. We will merely note that this is a new aspect of the problem, and one on which there is little data.

Effects of the features of the initial disturbance have received only cursory attention in this report. Only a rotating-stall-like disturbance was considered. Other possibilities also need study; disturbances which are statistically defined fluctuations, which arise from inlet distortions, asymmetric burner pulses, etc. are all possibilities for transient initiation, perhaps in combination with symmetric (surgelike) pulses arising either naturally or from control actions. Research on these questions of disturbance initiation should be helpful to guide experimental tests.

## Summary and Conclusions

1 An approximate theory has been developed for general post-stall transients in axial compression systems.

2 The analysis includes a two-dimensional, unsteady representation of the compressor flow field in the compressor annulus, together with a description of the overall dynamic response of the system. The resulting set of equations is thus capable of describing the strong coupling which can exist between surgelike and rotating-stall-like oscillations.

3 Examination of the coupled equations shows that surge and rotating stall can each exist in "pure" or equilibrium form; however, rotating stall cannot evolve without inducing some surgelike unsteadiness in the process. During either equilibrium surge or rotating stall, small amplitude disturbances of the other family will tend to die out.

4 Calculations have been carried out for general post-stall transients, which involve the growth or decay of rotating stall in the compressor. This growth or decay is calculated, along with the instantaneous system operating point. To the authors' knowledge, this is the first time that this has been done.

5 The instantaneous rotating stall-cell amplitude is found to have a significant effect on the instantaneous compressor pumping characteristic, and hence on the overall system response.

6 The theory extends previous analyses concerning the effect of the $B$ parameter ($B = (U/2a_s)\sqrt{V_p/A_cL_c}$) on post-stall transients, and adds details of the transient process: how rotating stall decays for large $B$ and how it evolves to a fixed level when $B$ is less than the critical value.

7 Other parameters besides $B$, in particular the compressor length to radius ratio $l_c = L_c/R$, can also have a strong effect on the system response. A limited parametric study shows that, for a given value of $B$, compressors of shorter length-to-radius ratio are more likely to exhibit surge than rotating stall. Initial conditions concerning stall-cell amplitude at the start of the transient may also be of importance, and should be studied.

8 The rotating-stall cell amplitude during unsteady flow is

different from that during steady-state operation in rotating stall. Consequently, the instantaneous compressor performance during a system transient can differ considerably from the characteristic measured during steady-state rotating stall.

9 The numerical results that are presented show qualitative agreement with the existing (but scarce) experimental data concerning the nature of the flow field during this type of transient.

10 Based on the results of the analysis, recommendations are made concerning future work on nonrecoverable stall.

## Acknowledgments

Most of the work described in the paper was carried out while the authors were in residence at NASA Lewis Research Center during the summer of 1983. The assistance of Mr. C. L. Ball in arranging this stay, as well as in providing a very conducive atmosphere for the research, is gratefully acknowledged. Additional support has also been provided by NASA under grant NSG-3208.

## References

1 Moore, F. K., and Greitzer, E. M., "A Theory of Post-Stall Transients in Axial Compressor Systems: Part I – Development of Equations," ASME Paper No. 85-GT-172.

2 Greitzer, E. M., "Surge and Rotating Stall in Axial Flow Compressors, Parts I, II," ASME JOURNAL OF ENGINEERING FOR POWER, Vol. 98, No. 2, Apr. 1976, pp. 190–217.

3 Greitzer, E. M., "The Stability of Pumping Systems—The 1980 Freeman Scholar Lecture," *ASME J. Fluids Eng.*, Vol. 103, June 1981, pp. 193–243.

4 Koff, S. G., and Greitzer, E. M., "Stalled Flow Performance for Axial Compressors-I: Axisymmetric Characteristics," ASME Paper No. 84-GT-93, 1984.

5 Koff, S. G., "Stalled Flow Characteristics for Axial Compressors," S. M. Thesis, Massachusetts Institute of Technology, Department of Mechanical Engineering, 1983.

6 Mani, R., "Compressor Post Stall Operation," *Lecture Notes from AIAA Professional Study Seminar on Airbreathing Propulsion*, G. C. Oates, course director, June 1982.

7 Day, I. J., "Axial Compressor Stall," Ph.D. Thesis, Cambridge University, Engineering Department, 1976.

8 Moore, F. K., "A Theory of Rotating Stall of Multistage Compressors, Parts I, II, III," ASME JOURNAL OF ENGINEERING FOR POWER, Vol. 106, No. 2, Apr. 1984, pp. 313–336.

9 Cumpsty, N. A., and Greitzer, E. M., "A Simple Model for Compressor Stall Cell Propagation," ASME JOURNAL OF ENGINEERING FOR POWER, Vol. 104, No. 2, Jan. 1982, pp. 170–176.

10 Wenzel, L., and Bruton, W. M., "Analytical Investigation of Non-Recoverable Stall," NASA TM-82792, 1982.

11 Peyret, R., and Taylor, T. D., *Computational Methods for Fluid Flow*, Springer-Verlag, New York, 1983.